On the External Effects Affecting Torsional Modes in Guide Vanes

International Journal of Fluid Machinery and Systems
Vol. 12, No. 2, April-June 2019

DOI: http://dx.doi.org/10.5293/IJFMS.2019.12.2.159
ISSN (Online): 1882-9554

Original Paper

On the External Effects Affecting Torsional Modes in Guide Vanes

Petter T K Østby[1,2], Eivind Myrvold[1], Jan Tore Billdal[1] and Bjørnn Haugen[2]

[1]Rainpower Norge AS, 2027 Kjeller, Norway,
petter.oestby@rainpower.no, eivind.myrvold@rainpower.no, Jan.Billdal@Rainpower.no
[2]NTNU, Richard Birkelands vei 2B, 7491 Trondheim, Norway, bjorn.haugen@ntnu.no

Abstract

Rotor stator interaction in high-head Francis turbines has led to several failures in recent years. Increasing efficiency demands require design optimization of the turbine components, which may lead to thinner profiles. Not only can component not withstand the given loads; quite often one or more of their natural frequencies coincide with that of the rotor-stator interaction. Most of the research published has been on runners, while other parts of the turbine are less studied. Even though guide vanes have torsional modes with frequencies which may be close to the exiting frequency from the rotor stator interaction with the runner, no significant failures due to resonance have been reported. This paper investigates some of the possible mechanisms which may negate resonance in the torsional modes of the guide vanes including; hydrodynamic damping from the flowing water and friction in the guide vane bearings. A case study is conducted on a guide vane where the calculated natural frequency is within 10% of the excitation frequency, while no significant vibrations have been reported. Further, the findings are generalized to Francis turbines of different specific speeds. The results indicate that the dynamics in the bearings are especially important to consider to be able to predict the vibration levels of the guide vane. Having the correct friction factor in the bearing may lead to significant damping and almost eliminate any excitation of torsional eigenmodes.

Keywords: RSI, guide vane, vibration, resonance

1. Introduction

In the last decade, several large high head Francis runners have experienced cracks. Through the work from several researchers [10, 4, 3] the cause of the failure have been contributed to a resonance in the runner with the pressure field created by the guide vanes. This interaction between the rotating runner and stationary guide vanes is called Rotor Stator Interaction (RSI). The guide vanes of the turbine will experience a similar transient pressure field from RSI as the runner, only in the stationary domain. This pressure field will create a torque on the guide vane stem, which in theory could excite a resonance with the torsional mode of the guide vanes. However, very few cases have been reported. Some pump turbines have reported torsional vibration at small openings due to self excitation from the flow field. Nenneman and Parkinsons [7] showed using advanced CFD how this phenomenon could be modeled. Predin et al. [8] found that a linear model for flow and the torsional movement of the guide vane was able to replicate measurements on a model pump turbine. Roth et al. [9] investigated the coupling of a bending mode in the guide vanes and the RSI pressure field. They showed how the RSI pressure amplitude decrease near the guide vane bending resonance frequency.

To estimate the risk of resonance the eigenfrequency of the torsional mode has to be calculated. The simplest way, and perhaps the common way, is to do a modal analysis where the guide vane is fixated at the arm, the bearings are modeled as friction less and the guide vane blade is submerged in water.

Using this method, we calculated the eigenfrequency of several old high head Francis turbine guide vanes in Norway. This study revealed that several of them had torsional frequencies within 10% of the exciting frequency from the runner. Even though such closeness between the forcing and eigenfrequency normally leads to large vibrations, none was observed in any of the turbines. In this article, we investigate what might be the cause to why no such vibrations have been observed. In particular, the effect of friction in the guide vane bearings have been investigated.

2. Theory

The vibrations of a complete regulating mechanism will be a set of complex and connected vibrations with several coupled modes. In

Received January 23 2019; accepted for publication April 1 2019: Review conducted by Yoshinobu Tsujimoto. (Paper number O19038S)
Corresponding author: Petter T K Østby, Petter.Oestby@Rainpower.no

* Part of this paper was presented at the 29th IAHR Symposium on Hydraulic Machinery and Systems, held at Kyoto, Sept. 16-21st, 2018.

this article, we consider the torsional vibrations of a guide vane as a single degree of freedom system with a characteristic natural frequency ω_n and damping ζ.

$$\ddot{x} + 2\omega_n\zeta\dot{x} + \omega_n^2 x = F(t) \quad (1)$$

As the guide vane increases the angular momentum of the water flowing from the stay vanes to the runner it experiences a force from the water. This normal force F_0 is balanced in the guide vane bearings together with a frictional force. The force $F0$ and friction force F_f will be in a stick condition when the frictional force is below the slip limit: $F_f = \mu \cdot F0$. μ is the frictional coefficient between the bearing and guide vane.

At the same time the guide vanes will be subject to a time varying pressure field due to the passing of the runner vanes. This pressure field will oscillate with the runner passing frequency $f_r = {}^{n_{rpm}}/_{60} \cdot Z_r$ and create an oscillating torque M on the guide vane. For high head Francis turbines, this will be the main excitation force of torsional movement of the guide vane. The guide vane is more or less fixated at the top. The dynamic torque on the blade will twist the guide vane stem, rotating it inside of the bearings.

This configuration results in three different physical conditions in the interaction between the guide vane stem and the bearing. These are presented below.

2.1 Guide Vane stem rolling in bearing

If the dynamic torque, M, is significantly less than the frictional slip torque, M_f, in the bearings ($M << r \cdot \mu \cdot F0 = M_f$), the guide vane stem will be stuck to the bearing and not be able to slide. Given that guide vane bearing has a radius R which is larger than the stem radius r, the guide vane stem will roll back and forth in the bearing. This is similar to a cylinder rolling back and forth in a valley under the force of gravity.

This case can be modeled as a cylinder rolling inside of a larger cylinder while being statically loaded with $F0$. The setup can be seen in Fig. 1. In Figure 1 the guide vane stem has rotated an angle of φ. Since there is no sliding, the distance rolled on the bearing has to be the same as for the stem.

$$R \cdot \theta = r \cdot (\theta + \phi) \quad (2)$$

As the normal force $F0$ now acts outside of the contact point P it will create a restoring torque Mr forcing the stem back to the equilibrium position. This torque is found by calculating $F0$'s torque around point P and linearizing which gives

$$M_r = \frac{F_o \cdot r^2}{\Delta r}\phi \quad (3)$$

where Δr is the radial clearance in the bearing. This restoring torque is proportional to the angle θ and this represents an additional stiffness (in addition to the stem torsional stiffness) resisting the vane rotation. The formula reveals that the stiffness is inversely propositional to the clearance in the bearing. Given that such bearings often have tight clearances this spring constant may be significant.

It is worth noting that this calculation is done with the assumption of a perfectly circular stem and bearing. Wear and machining inaccuracies will change the shape, which can affect the calculated stiffness.

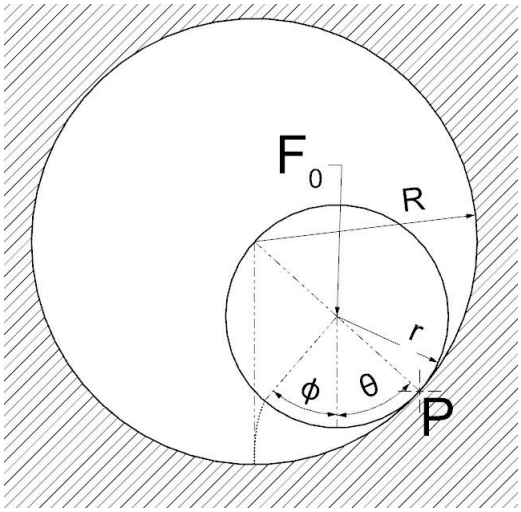

Fig. 1 Sketch of the guide vane stem inside of the bearing. Shown in a pertubated position after rotating an angle φ. Difference in diameter is greatly exaggerated.

2.2 Guide Vane stem sliding in bearing

If the dynamic torque is significantly larger than the frictional slip torque ($M >> M_f$) the guide vane stem will slide inside of the bearing. In this case, the friction will act as damping. The amount of equivalent viscous damping (ζ_{eq-dry}) produced by such dry friction is dependent on both the excitation frequency (ω) and the amplitudes of the motion (A).

$$\zeta_{eq-dry} = \frac{2\mu F_o}{\pi m \omega \omega_n A} \tag{4}$$

As the vibration amplitude is in the denominator of the equation, the equivalent damping will diminish as the amplitudes grow.

2.3 Guide Vane stem rolling and sliding in bearing

If the dynamic torque is above the frictional slip torque, but still in the same order of magnitude ($M > M_f$), the resulting motion will be a combination of sliding and rolling. When the dynamic torque is below the frictional stick limit, the guide vane will roll, but as soon as the torque increases above the frictional stick limit, the guide vane will slide back with the friction acting as a damper. In this case the spring/damping effect of the bearing becomes non-linear and cannot be analyzed analytically. To solve this a numerical approach has to be utilized. We can however estimate the friction coefficient giving the greatest amount of damping. The damping work of the bearing is equal to the integral of the area traced out by the motion of the stem in the bearing as shown in a $M - \theta$ diagram. Fig. 2 shows a schematic of the hysteresis in the bearing.

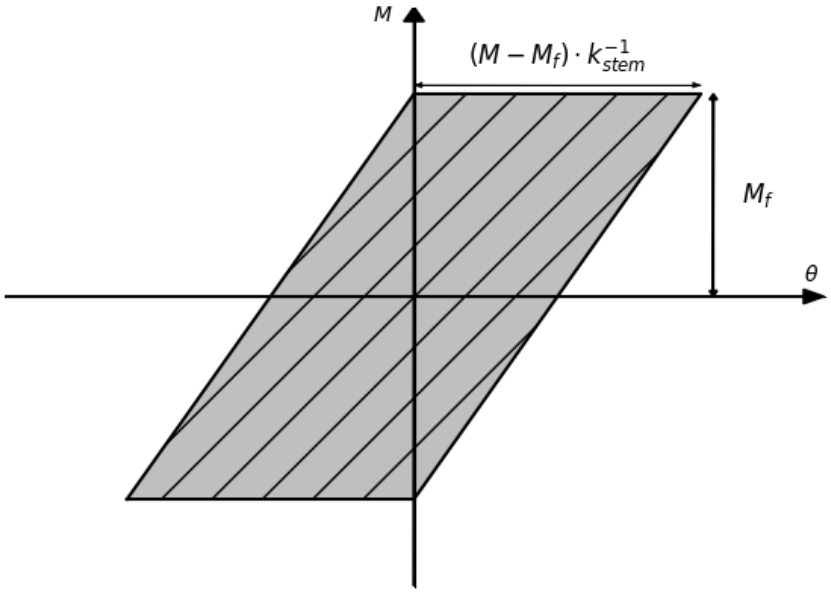

Fig. 2 Motion of the stem in the bearing with the rolling/sliding configuration. The area in grey gives the damping work in the bearing.

From Fig. 2 we can conclude that the damping work will be

$$W_b = 2 \cdot M_f \cdot \left(M - M_f\right) \cdot k_{stem}^{-1} \tag{5}$$

The maximal work can be found by differentiating eq. (5) with respect to the frictional torque:

$$M_f = \frac{M}{2} \tag{6}$$

Thus, when the maximal frictional slip torque in the bearing is half of the dynamic torque we expect the greatest amount of damping. This is a simplified analysis as it ignores the dynamics of the guide vane mass and oversimplifies the dynamics of the bearing, however, as will be shown later, it gives a decent estimate.

2.4 Hydrodynamic damping

Research by Carl et al. [1] and Cotou et al. [2] has shown that the hydrodynamic damping for a vibrating foil may be significant at high water velocities. As the velocity of the water may reach 60 to 70 $^{m}/_{s}$ at the trailing edge of the guide vane this phenomenon must be accounted for to predict the guide vane motion.

Using the modal work method developed for a hydrofoil by Monette et al. [5], and adapted for guide vanes by Myrvold [6], the damping can be expressed as in eq. (5). It takes the work (W_f) done by the water through a vibration cycle and scales it based on the frequency (ω_n), mass(m) and amplitude(A) of the eigenmode in question.

$$\zeta = \frac{W_f}{2\pi \cdot m \cdot \omega_n^2 \cdot A^2} \tag{7}$$

2.5 Hydrodynamic stiffness

Monette et al. [5] provides compelling arguments that the added stiffness from the water flow is insignificant and the analytical formulas to calculate this effect is quite complicated. However, in the case of torsional movement of the guide vane it is easily available.

When dimensioning the guide vane apparatus, it is important to know the relation between the hydraulic torque and guide vane opening. As the torsional motion of the guide vane blade is the same as changing the guide vane opening, the hydrodynamic stiffness can be read directly from the M_{hydro}-θ diagram.

$$k_{hydro} = \frac{dM_{hydro}}{d\theta} \tag{8}$$

3. Case Study

To investigate the effect of the bearing on the natural frequency of a guide vane a case study was conducted on a high head Francis turbine. This particular turbine was chosen as the calculated natural frequency of the torsional mode of the guide vane is near the runner passing frequency (when assuming only stem torsional stiffness). As it is a high head Francis the dynamic torque applied to the guide vanes are estimated to be higher than on a low head turbine. The main data of the turbine is shown in Table 1.

Table 1 Turbine Data

Rated Head	:	395	m
Speed	:	500	rpm
Number of Runner Vanes	:	32	pc
Speed Number	:	0.063	n_{QE}
Runner Passing Frequency	:	267	Hz

The guide vane stem is long and slender with three bearings. A sketch of the geometry is shown in Fig. 3. The bearing/stem have a h8/E7 fit which give a radial clearance of $0.036 < \Delta r < 0.08$. A CFD calculation of the turbine in question reveals a static force F_0 on the guide vanes vary from $99kN$ at speed no load to $58kN$ at full load. The dynamic torque amplitude is calculated to be about $M = 48Nm$ for all loads. Using a lower bound estimation of the friction coefficient, $\mu = 0.05$, gives a minimum frictional torque of $M_f = 130Nm$. As the dynamic torque is significantly less the frictional torque the guide vane stem should thus roll in the bearing.

Using eq. (3) we can now calculate the possible range of stiffness from the bearings. Comparing this to the torsional stiffness of the stem, eq. (7), gives an estimate of the importance of the bearing stiffness. Here the Young Modulus (E), diameter of the stem (D), length (L) and poisson factor (ν) are the important parameters.

$$k_{stem} = \frac{dM}{d\theta} = \frac{GI_p}{L} = \frac{E \cdot \pi \cdot D^4}{2(1+\nu) \cdot 64 \cdot L} \tag{9}$$

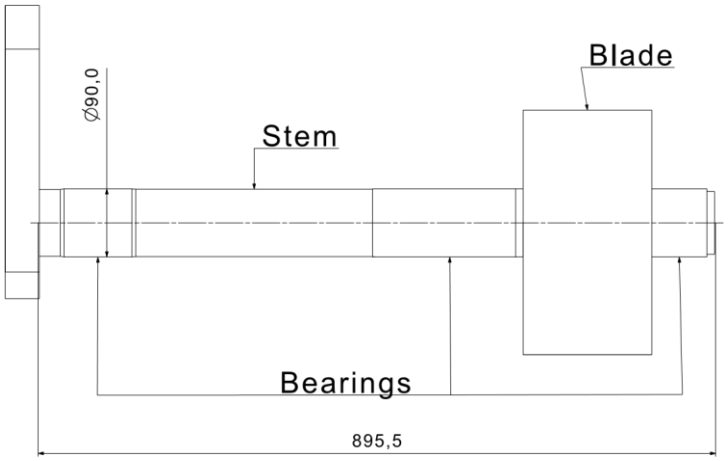

Fig. 3 Sketch of Guide vane geometry

Table 2 Torsional stiffness k_θ.

$Bearing_{max}$	:	$5.6 \cdot 10^6$	$Nm/_{rad}$
$Bearing_{min}$	:	$1.48 \cdot 10^6$	$Nm/_{rad}$
Guide vane stem	:	$8 \cdot 10^5$	$Nm/_{rad}$

As the stiffness from the bearings is of the same order of magnitude as the guide vane stem, their effect cannot be disregarded when calculating the natural frequency of the guide vanes.

3.1 Numerical Investigation

To evaluate the guide vanes torsional response to the RSI pulsations from the runner a set of numerical calculations were conducted.

3.1.1 Eigenfrequency

The eigenfrequency of the guide vane is calculated using the range of possible bearing stiffnesses. A water volume is placed around the guide vane profile to include the added mass effect of the water. Assuming that the static load F0 mainly is carried by the two bearings closest to the blade, half of the bearing stiffness is distributed to each of those bearings.

With frictionless bearings the natural frequency of the guide vane is calculated to be 245 Hz, only 8% away from the exciting frequency. However, including the bearing stiffness significantly increases the natural frequency. This is shown in Fig. 4 where the effect of bearing stiffness becomes evident. The torsional frequency increases 50% to 125% depending on operating point and clearance.

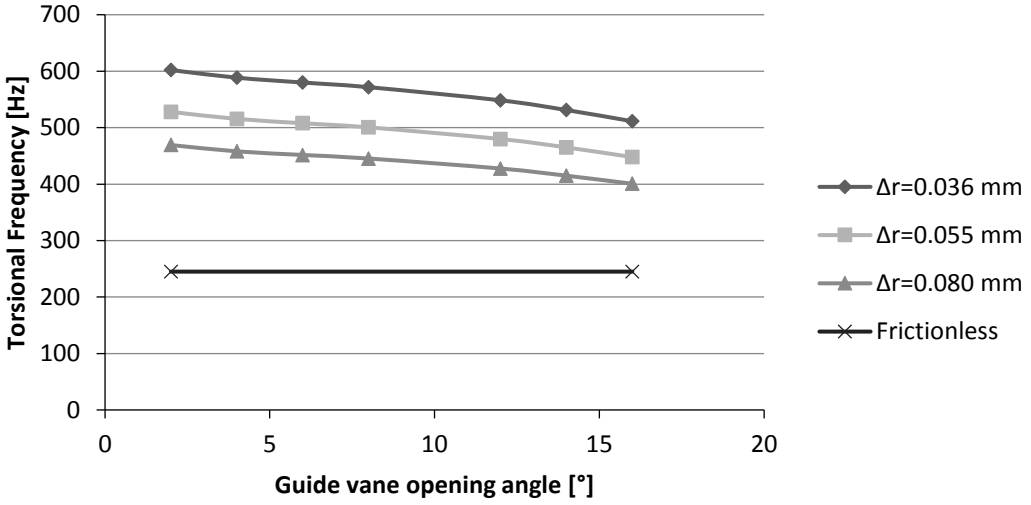

Fig. 4 Torsional frequency of guide vane with and without bearing stiffness for different bearing clearances Δr and different operating points

3.1.2 Hydrodynamic damping

Using a transient CFD calculation with imposed vibration of the guide vane blade according to the eigen modes and frequencies found above, the damping was calculated using eq. (7). Only the modes and frequencies with a radial clearance of 0.055mm was used. The guide vane was forced to oscillate with two different amplitudes, 0.1mm and 0.01mm.

As a simplification, all guide vanes were forced to oscillate in phase with the neighbour vane. This is not physically correct, but including the phase shift would significantly increase the computational requirements. The resulting damping is almost constant at 3% with an increase at very small openings.

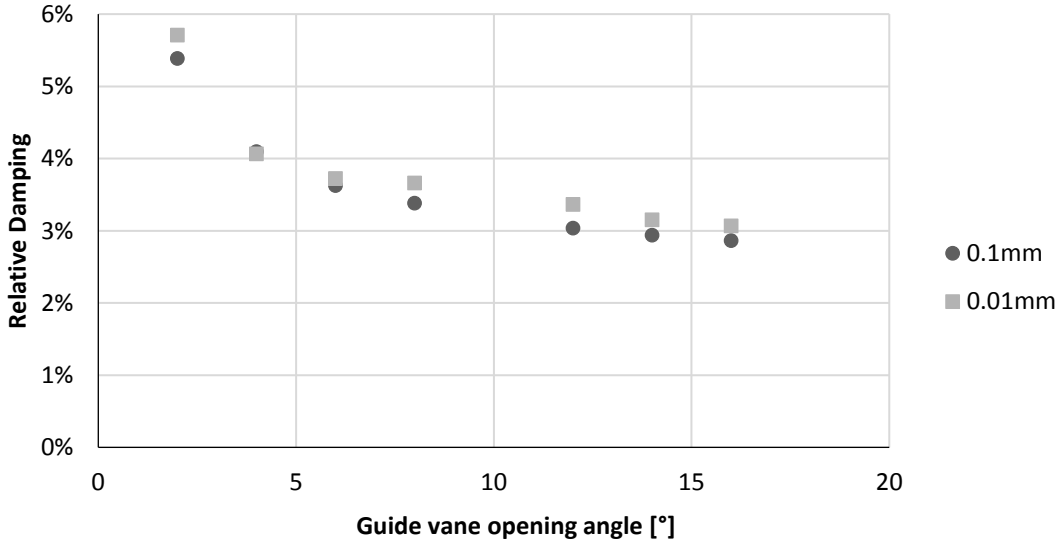

Fig. 5 Relative Damping (ζ) calculated for the torsional mode of the guide vane at different openings with two motion amplitudes.

3.1.3 Hydrodynamic Stiffness

Using the hydraulic torque diagram, the hydrodynamic stiffness was calculated with eq. (8). The value ranges from $-2 \cdot 10^{4Nm}/_{rad}$ to

$0^{Nm}/_{rad}$. Even though the damping is negative at all openings, its value is insignificant compared to both the stem stiffness and bearing stiffness. It is thus not included in the model.

3.1.4 Harmonic Response

To quantify the difference between guide vane bearings with infinite friction $(M_f/M = \infty)$ and without friction $(M_f/M = 0)$ a harmonic response analysis was conducted at the runner vane passing frequency (266.67[Hz]). A harmonic pressure field from a transient CFD analysis was used as the forcing field on the guide vane blade. A constant damping of 3% is used as calculated above. Figure 6 shows the results where the stiffness from the bearings reduce the amplitudes by more than a decade.

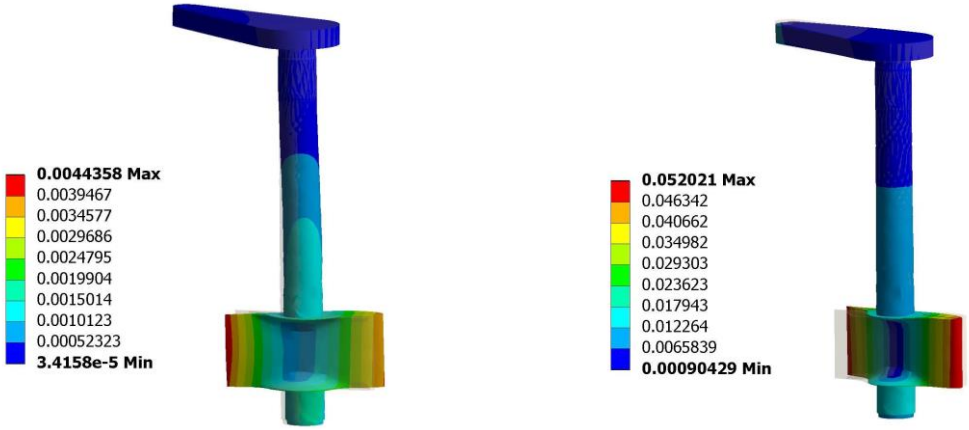

Fig. 6 Vibration Amplitude with stem rolling in bearing (left) and frictionless sliding in bearing (Right).

3.1.5 Rolling and sliding bearing

To investigate the effect of slip stick motion with rolling and sliding in the bearing $(0 < \frac{M_f}{M} < \infty)$ a simplified transient model of the guide vane system was created. It consists of four linear torsional elements. Each torsional stiffness and moment of inertia was extracted from the FE-model used in the harmonic response analysis. A stick-slip spring was added to each guide vane stems at the bearings, modelled according to eq. (11) as described by Dahl [11]. The force F0 is assumed to be equally distributed in each bearing giving each a slip force of $M_f/2$ and a spring constant of $k_\theta = 1.5 \cdot 10^6\ N/rad$. The harmonic torque from CFD, $M(t)$, is applied to the blade. Further, the damping force calculated in section 0 was also added to the blade. A schematic representation is shown in Fig. 7 and the results are shown in Fig. 8. The system is solved using the "lsoda" solver [12].

$$\frac{dM_r(\theta)}{dt} = k_\theta \left| 1 - \frac{M_r}{M_f}\, sgn(\dot{\theta}) \right|^i sgn\left(1 - \frac{M_r}{M_f}\, sgn(\dot{\theta}) \right) \cdot \dot{\theta} \tag{10}$$

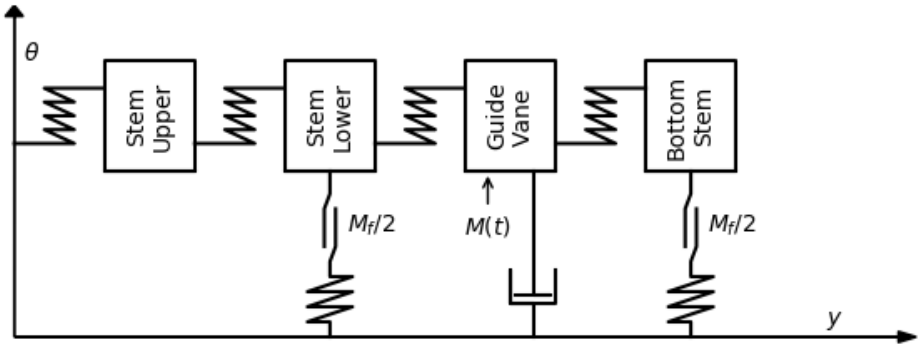

Fig. 7 Schematic of model used for stick slip calculation

By calculating the friction work in each of the bearings and relating it to the maximal potential energy in the system, we can get an estimate for the relative damping from the bearings using eq. (11).

$$\zeta_b = \frac{1}{4\pi} \frac{W_b}{EP} \tag{11}$$

The figure below clearly shows the transition between the two eigen frequencies as the stiffness of the bearing becomes more dominant with greater frictional slip torque. We also see that a relative bearing slip torque between 0.7 and 2.0 gives the smallest vibration amplitudes. For almost all slip torques will the friction in the bearing be significant and dominate over the hydrodynamic damping.

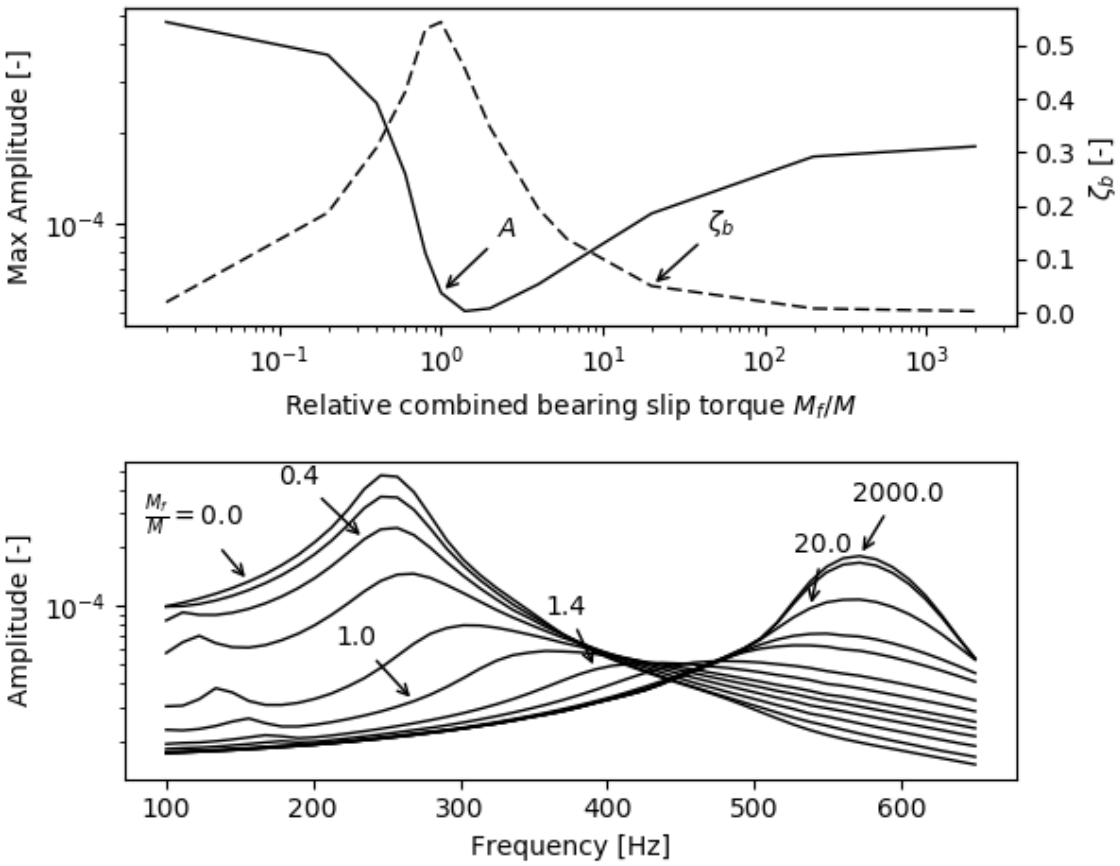

Fig. 8 Vibration amplitudes for different relative slip torques, Mf/M, in the bearings. Bottom: Frequency response diagram of the system for selected relative friction slip torques. Top: Maximal vibration amplitude ($\boldsymbol{A}$) and average damping ($\boldsymbol{\zeta_b}$) in the bearings over all frequencies for selected friction slip torques.

3.2 Measurements

To investigate the dynamics of the guide vane a measurement series was conducted on the reference turbine. Ideally, one should either measured the stresses in the guide vane stem or the acceleration on the guide vane blade. These areas are however not available during operation. Two accelerometers was instead placed on the guide vane arm as shown in Fig. 9. The vibration data was logged at 4800[Hz].

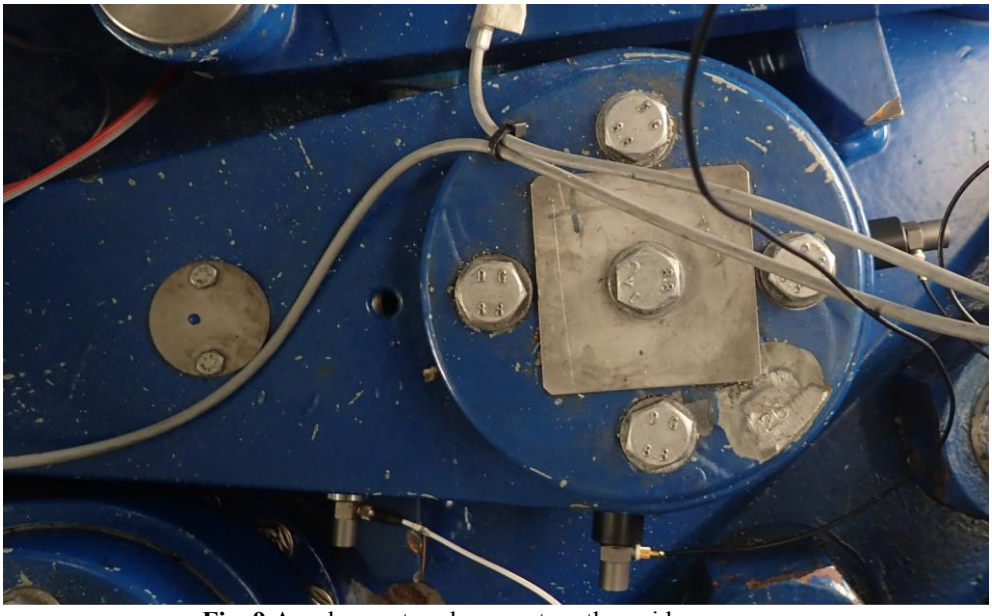

Fig. 9 Accelerometer placement on the guide vane arm

The overall measured vibration levels was small. By extracting the frequency component of each measurement at the runner vane passing frequency it is possible to compare the measurements to the Harmonic Response analysis. The results are shown in Fig. 10. It clearly shows that the effect of the bearing stiffness due to friction has to be taken into account. Without this stiffness the calculated

vibration amplitudes become too high. Including the bearing stiffness without sliding ($M_f = \infty$) gives a result very close to the measured values. The measured values are not compared to the calculated values from the stick-slip bearing model, as the model is too simple to capture the actual movement of the accelerometers.

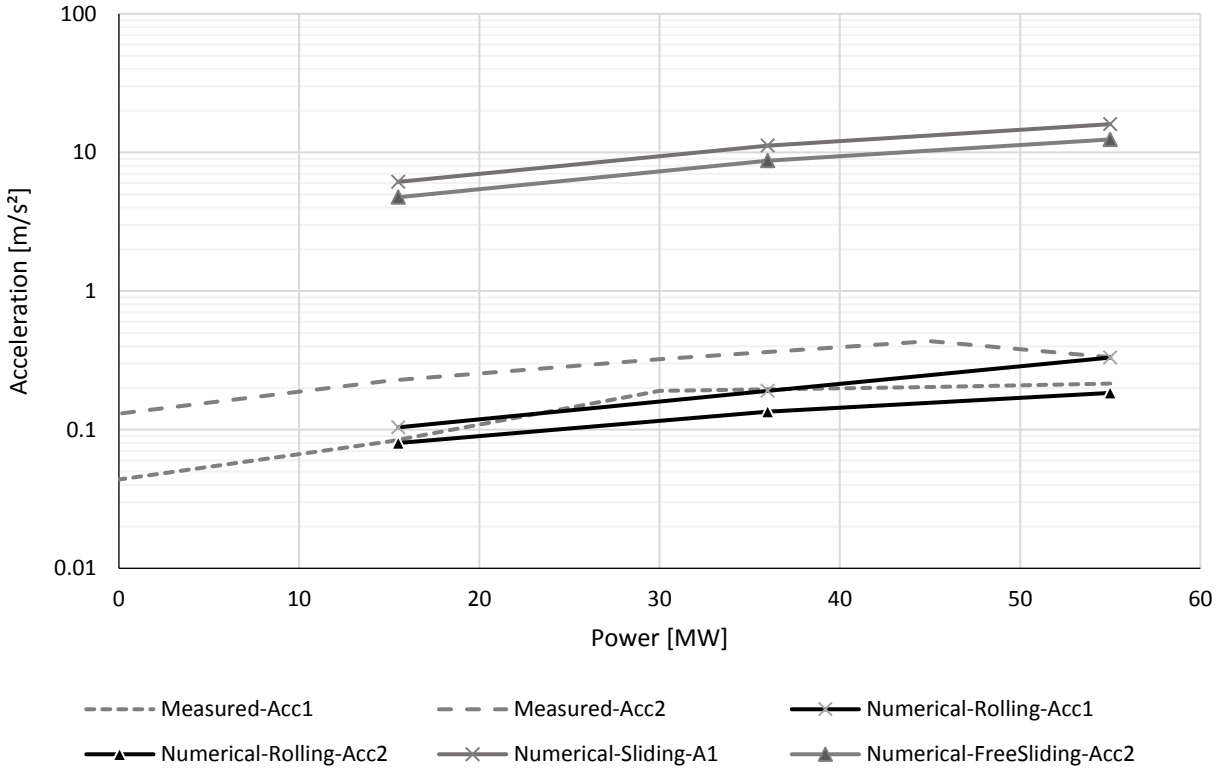

Fig. 10 Measured Accelerometer data vs calculated values with rolling and sliding bearings

4. Applicability for other turbines

The case study showed that for a high head Francs turbine the guide vane will most likely roll in the bearings and the bearing stiffness is significant compared to the torsional stiffness of the guide vane.

Using data from numerical simulations of other Francis turbines, the required bearing friction coefficient that gives $M_f/M = 1$ has been calculated. Nineteen different turbines was included in the set. Some with several operating points. The result is shown in Fig. 11. In none of the cases examined does the required friction coefficient exceed 0.05. This seem to be independent of the turbine head. This will of course be somewhat dependent on the design of the guide vane. However, this diagram contains data from both new and old designs.

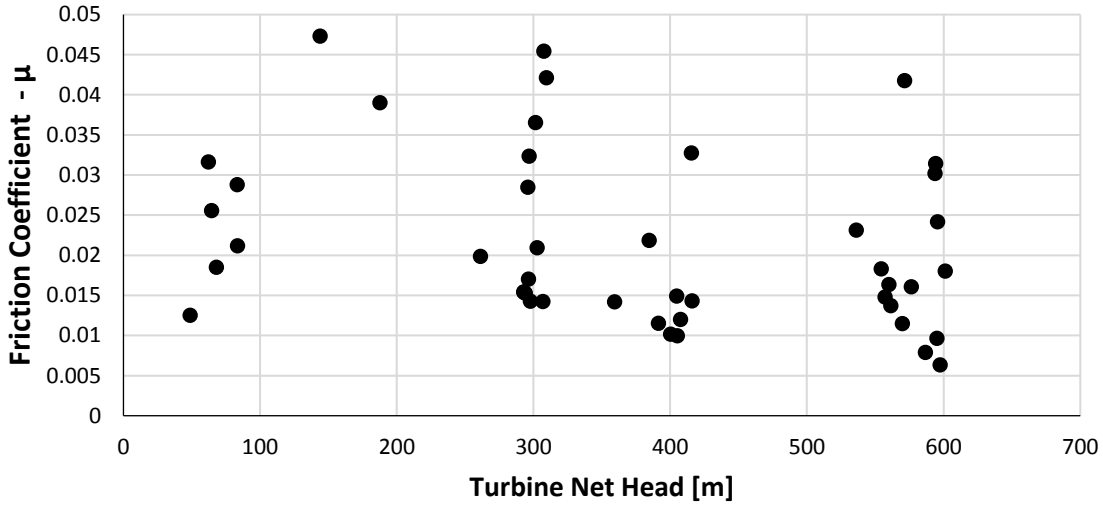

Fig. 11 Required bearing friction coefficient to give $\boldsymbol{M_f/M = 1}$

The relative stem stiffness to the bearing stiffness is shown in Fig. 12. It shows a clear trend where the bearing stiffness dominates at high heads while at low head turbines the stem stiffness is dominating.

Even though the effect of bearing stiffness is reduced at low head turbines, the effect is still significant enough to change the torsional frequency and it should thus be included in eigenfrequency calculations for all turbines.

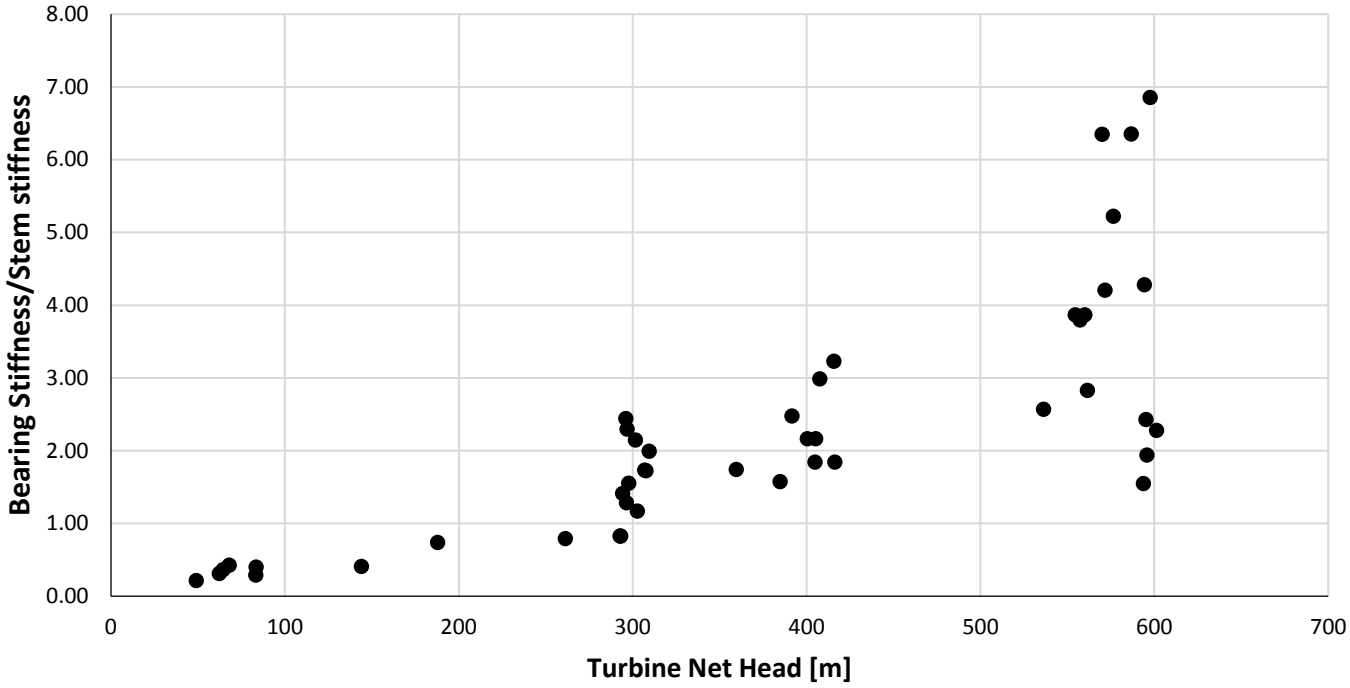

Fig. 12 Bearing stiffness divided by stem stiffness assuming 0.1mm radial clearance for different turbines.

5. Conclusion

When estimating the harmonic response of the torsional eigenmode of guide vanes in Francis turbines, it is important to include the effect the bearings has on the relevant eigenfrequency. This was verified through on site measurements. As there is a small clearance in the bearing, the bearing will have a torsion-spring like behaviour forcing the guide vane back to its base position when pertubated by an external torque. This effect is very dependent on net head. For very high head units the spring coefficient of the bearing can be 2-10 times the torsional stiffness of the guide vane stem. For low head units the guide vane stem is significantly more torsional stiff than the bearings. The added stiffness from the bearings increases the natural frequency of the torsional mode significantly compared to the estimated value using frictionless bearings. Due to the close relation between the bearings clearance and the stiffness, guide vanes with worn bearings will most likely have different torsional eigenfrequencies than new guide vanes.

For none-infinite friction coefficients in the bearing, there will likely be a combination of rolling and sliding. This combination causes a non-linear stick-slip phenomenon, which removes energy from the oscillating system. Using a transient numerical model we showed how the natural frequency transitions from a low value to a higher value with increasing coefficient of friction. In between, the frictional work will dampen the oscillations creating the smallest amplitudes when the frictional torque is about the same as the external torque. Based on the analysed turbines, this stick-slip phenomenon will probably occur on turbines of all net heads.

A high head francis turbine was used as a case study. Here we found that the bearing stiffness doubled the natural frequency of the guide vanes. The hydrodynamic damping was found to be in the range of 3%-6% and the frictional damping in the bearings in the range of 10%-50%. With such significant damping and extra stiffness from the bearings it is not surprising that no significant vibrations were measured on the unit. Whether or not the same will apply for low head units have not been directly investigated, but it is likely that bearing dynamics will affect the torsional modes also for these turbines.

Nomenclature

μ	Coefficient of friction	[-]	Mr	Restoring torque by bearing on stem	[Nm]
A	Vibrational amplitude	[rad]	r	Guide vane stem radius	[m]
D	Diameter of stem	[m]	R	Guide vane bearing rad	[m]
E	Youngs' modulus	[-]	W	Work	[J]
EP	Potential Energy	[J]	ζ	Relative damping	[-]
$F0$	Static force on guide vane	[N]	v	poisson factor	[-]
k	Spring torsional stiffness	[Nm/rad]	φ	Angular rotation of guide vane	[rad]
L	Length of stem	[m]	ω	Excitation frequency	[rad/s]
M	External torque	[Nm]	ω_n	Eigen frequency	[rad/s]
Mf	Frictional slip torque	[Nm]			

References

[1] Carl W. Bergan, Bjørn W. Solemslie, Petter Østby, and Ole G. Dahlhaug. Hydrodynamic damping of a fluttering hydrofoil in high-speed flows. International Journal of Fluid Machinery and Systems, 11(2):146– 153, 2018.
[2] A Coutu, C Seeley, C Monette, B Nennemann, and H Marmont. Damping measurements in flowing water. IOP Conference Series: Earth and Environmental Science, 15(6):062060, 2012.
[3] Andre Coutu, Roy MD, Monette C, and Nennemann B. Experience with rotor-stator interactions in high head francis runner. Proceedings of the 24th IAHR symposium on hydraulic machinery and systems, page 10, 2008.
[4] Eduard Egusquiza, Carme Valero, Quanwei Liang, Miguel Coussirat, and Ulrich Seidel. Fluid added mass effect in the modal response of a pump-turbine impeller. (48982):715–724, 2009.
[5] C Monette, B Nennemann, C Seeley, A Coutu, and H Marmont. Hydro-dynamic damping theory in flowing water. IOP Conference Series: Earth and Environmental Science, 22(3):032044, 2014.
[6] Eivind Myrvold. Numerical analysis of rotor-stator interaction in a francis turbine guide vane. Master's thesis, Norwegian University of Life Sciences (NMBU), 2017.
[7] B Nennemann and E Parkinson. Yixing pump turbine guide vane vibrations: Problem resolution with advanced cfd analysis. In IOP Conference Series: Earth and Environmental Science, volume 12, page 012057. IOP Publishing, 2010.
[8] Andrej Predin. Torsional vibrations at guide-vane shaft of pump turbine model, 1997.
[9] Steven Roth, Vlad Hasmatuchi, Francisco Botero, Mohamed Farhat, and Francois Avellan. Influence of the pump-turbine guide vanes vibrations on the pressure fluctuations in the rotor-stator vaneless gap. In
[10] Proceedings of the 4th International Meeting on Cavitation and Dynamic Problems in Hydraulic Machinery and Systems, number EPFL-CONF-167186, 2011.
[11] Chirag Trivedi and Michel J. Cervantes. Fluid-structure interactions in francis turbines: A perspective review. Renewable and Sustainable Energy Reviews, 68(Part 1):87 – 101, 2017.
[12] Philip R. Dahl. "Solid Friction Damping of Mechanical Vibrations," AIAA Journal, Vol. 14, No. 12 (1976), pp. 1675-1682.
[13] L. Petzold, "Automatic selection of methods for solving stiff and nonstiff systems of ordinary differential equations," SIAM Journal on Scientific and Statistical Computing, Vol. 4, No. 1, pp. 136-148, 1983.